METHOD OF DETERMINING NON-LINEAR TEMPERATURE DISTRIBUTION ACROSS THE THICK PLATE THICKNESS THAT SIMPLIFIES NUMERICAL CALCULATIONS

by

Vesna O. MILOŠEVIĆ-MITIĆ[a], Ana S. PETROVIĆ[a*], Nina M. ANDJELIĆ[a], and Aleksandar R. BOGOJEVIĆ[b]

[a] Faculty of Mechanical Engineering, University of Belgrade, Belgrade, Serbia
[b] Institute of Physics, University of Belgrade, Belgrade, Serbia

Original scientific paper
https://doi.org/10.2298/TSCI240705262M

In this paper thermal loading of plate elements under several different heat sources (sinks), while sources are defined by the power and time of action, is considered. The heat sources are placed on the plate element sides parallel to the middle plane, while lateral sides are thermally insulated. Firstly, the dynamic problem was solved in closed analytic form using the technique of integral transformations. While discussing numerical examples that represent establishment of a non-linear distribution of temperature across the thickness of the element, laws on the basis of which this distribution can be calculated relatively simply without solving differential equations are established. Based on that idea, for steel elements, two basic diagrams were formed, which represent the procedure for calculating the temperature distribution. The procedure defined in this paper is suitable for simplifying the procedure of deformation and stress calculations of some real thermal loaded structures, using the finite element method.

Key words: *temperature, temperature distribution, integral transformation, heat source, thick plate, stress*

Introduction

A large number of mechanical engineering and civil engineering structures, made of different materials, are loaded both with mechanical and thermal loads during their work life. Thermal load of nuclear and chemical reactors, steam boilers, heat exchangers, concrete dams, satellites*, etc.* has an extremely large influence on their structural behavior. Most of thermally loaded constructions have extremely complex geometry, so the finite element method (FEM) has to be used in numerical calculations. Most thermally loaded structures are represented by models made of thin and thick plates and shells. Depending on the type of these structures, the analytical determination of the temperature field can be very complicated. Seddiq and Maerefat [1] the solution of the heat transfer problem in the plates and channels of the heat exchanger is shown. The corresponding PDE were solved using the separation of variables method and a solution was obtained that explicitly defines the temperature fields. Gaćeša *et al*. [2] and Rajić *et al*. [3] the significant influence of thermal load on the behavior of fire-tube boilers is shown. Due to the complexity of the structures, FEM was applied to determine stresses and strain field of the structure. Calculation of thermal stresses in low alloy steels is presented in [4],

* Corresponding author, e-mail: aspetrovic@mas.bg.ac.rs

where the authors considered physics-based models where each point in the numerical model is volume with micro-structure. Variation of temperature along the length of the aluminum fins for aerospace applications are presented in [5]. In the process of laser forming of thin plates, non-uniform thermal stress is induced. The temperature gradient mechanism is studied in [6] to obtain deformation of a plate in that process. Thermal load acting on thin plates can contribute to their bending, buckling and curling. Murphz and Ferreira [7], the determination of the flat plate buckling temperature is analyzed and it is shown that the obtained results are in a good agreement with the experimental values. Bending of annular sector plate under the influence of thermal load is shown in [8]. The thermal moment is obtained based on the temperature field, and a numerical example is given for an aluminum plate. Theoretical model for non-linear analysis of thin rectangular plates subjected to transverse mechanical loads and to thermal gradients, based on large deformation theory is developed in [9]. The study of heat conduction in a half space of materials, whose thermal properties depend on temperature, is presented in [10], and it is highlighted that the obtained results are in a good agreement with the FEM results. Thermo-elastoplastic analysis of bending of plates, made of functionally graded materials (FGM), under the influence of both mechanical and thermal loading is analyzed in [11], using a novel meshless approach. The bending of thin and thick FGM plates is considered in [12] by applying the classical theory of thermoelasticity. Material constants are defined as corresponding continuous functions of position. For plates and shells made of non-metals that have a low heat conduction coefficient, the temperature distribution across the thickness is very important. Thermoelastic vibrations of functionally graded plate of silicon material subjected to thermal load is shown in [13]. The bending of metal and concrete plates depending on the temperature gradient is shown in [14], using analytical and numerical procedures. The temperature field has an extremely large influence on the stress and deformation field of structures that work under the influence of variable electromagnetic load. The mathematical model that describes the temperature field during high frequency induction heating, shown in [15], considers the influence of a large number of heating parameters and gives a good agreement with experimental values. Milošević-Mitić *et al.* [16] defines the dynamic behavior of a thin plate under the influence of a moving high frequency inductor, where the temperature field is determined by applying an analytical calculation using the method of integral transformations. The same method was applied to consider the temperature field in a conductive strip subjected to quasi-steady electromagnetic field, [17]. The heating of a bimetallic plate subjected to electromagnetic field tangential to the plate is described in [18], and the temperature field caused by the action of high frequency electromagnetic waves is described in [19]. To solve differential equations that describe problems of this type, the method of integral transformations is most often used, especially Laplace and Fourier transforms. The great importance of this method is described in [20]. Laplace transform procedure, applied for obtaining analytical solutions for deflection and temperature of rotating nanobeams subjected to variable harmonic heat source and dynamic load with exponential decay, was presented in [21]. Thermal stress and strain rates in a thick walled rotating cylinder was studied in [22].

The main goal of this paper is to determine the temperature field of thin and thick plate elements under the influence of heat sources placed on plate element sides parallel to the middle plane. The power of these sources can be determined through the intensity of the heat conduction vector. The problem formulated in this way is consistent with the problem of heating a metal plate under the influence of a high frequency electromagnetic wave, when the penetration depth is negligible and when the conductor absorbs the entire power of the wave on the surface itself. Its strength can be determined by the Poynting vector. By analyzing the

obtained results, a relatively simple way of calculating the temperature field was observed, and within this paper, diagrams corresponding to steel elements are given. For other materials, corresponding diagrams could be formed in the same way.

Mathematical model of the problem

Consider a plate element of dimensions $a \times b \times h$ placed in the Cartesian co-ordinate system (x, y, z) as shown in fig. 1. Since this consideration does not apply to thin plates only, the co-ordinate axes are placed along the edges of the plate, and not in its middle plane. Let all four lateral sides be thermally insulated, and heat exchange takes place only through the upper and lower parallel plane, that is, for $z = 0$, h. This heat exchange can be described in two ways, through Fourier's law or by placing surface heat sources.

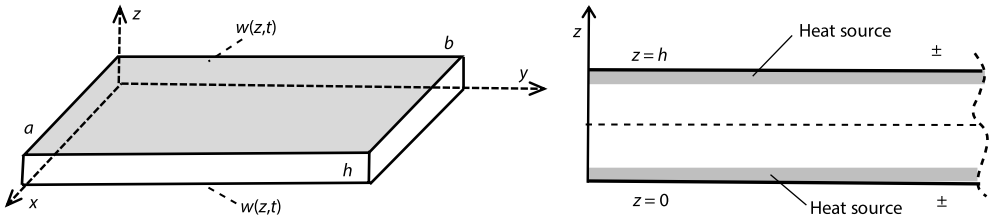

Figure 1. Rectangular plate $a \times b \times h$ in Cartesian co-ordinate system (x, y, z)

The systems of equations describing the temperature field and the deformation field are generally coupled, but for most materials used in mechanical engineering, the coupling co-efficient is small and can be neglected. The equation describing the temperature field in a plate, for the uncoupled problem:

$$\left(\frac{\partial^2}{\partial x^2}+\frac{\partial^2}{\partial y^2}+\frac{\partial^2}{\partial z^2}-\frac{1}{\kappa}\frac{\partial}{\partial t}\right)\theta(x,y,z,t)=-\frac{1}{\lambda}\sum_{i=1}^{n}\underline{w}_i(x,y,z,t) \tag{1}$$

where κ is the coefficient of thermal intensity, λ – the heat conduction coefficient, and t – the time. Temperature field is presented as θ [°C or K] = $T - T_0$ where T_0 is the temperature of the plate in its natural state. The quantity of heat generated in a unit volume and unit time (heat source intensity) is represented as $\underline{w}_i$. In the analysis that follows, the term temperature will refer to the change in the temperature of the element θ comparing to its natural state.

When the sides of the plate are thermally insulated, and when the heat exchange takes place over the entire upper and lower side, the temperature distribution depends only on the co-ordinate perpendicular to the middle plane, z. In order to define the conditions under which a non-linear or linear temperature distribution is established, two cases of thermal load will be observed:

– surface sources (sinks) of heat of power w_i ($i = 1,\ldots, k$) [Wm^{-2}] are placed on the lower and upper sides of the plate (sources can also be defined through Fourier's law), and
– the temperatures on the upper and the lower plane of the plate are constant.

Surface heat sources (sinks) are placed on the upper and lower parallel side of the plate

In fig. 1 a part of the observed plate (plate thickness, h), as well as the adopted position of the z-axis is shown. If only the temperature change in the direction of the z axis is observed, the heat conduction eq. (1) takes the form:

$$\left(\frac{\partial^2}{\partial z^2}-\frac{1}{\kappa}\partial t\right)\theta(z,t)=-\frac{w(z,t)}{\lambda} \tag{2}$$

Let the total temperature load of the plate $w(z, t)$ consist of several heat sources (k sources in total) that can be represented:

$$w_i(z,t)=w_i\delta(z-a_i)\left[H(t-t_{\mathrm{is}})-H(t-t_{\mathrm{ie}})\right],\ i=1...,k \tag{3}$$

where w_i is the intensity of the heat source, a_i – the indicates the position of the source in relation the z-axis, t_{is} – the time when the source work is starting, and t_{ie} – the time when the heat source work stops. The $H(t)$ is the Heaviside function and $\delta(z)$ is the Dirac function. The equation that describes the temperature distribution dependence on the co-ordinate z and time t:

$$\left(\frac{\partial^2}{\partial z^2}-\frac{1}{\kappa}\partial_t\right)\theta(z,t)=-\frac{1}{\lambda}\sum_{i=1}^{k}w_i\delta(z-a_i)\left[H(t-t_{\mathrm{is}})-H(t-t_{\mathrm{ie}})\right] \tag{4}$$

Since in this consideration the heat sources are placed at positions $z = 0$ and $z = h$, the boundary conditions on the upper and the lower plate plane have the form:

$$\left.\frac{\partial\theta}{\partial z}\right|_{z=0,h}=0 \tag{5}$$

In accordance with the problem previously described and defined, the differential eq. (4) is solved by applying the finite Fourier cosine transform defined:

$$\theta_c(n)=\int_0^h\theta(z)\cos\alpha_n z\mathrm{d}z,\ \alpha_n=\frac{n\pi}{h} \tag{6}$$

and eq. (4) is obtained in its transformed form:

$$\left(-\alpha_n^2-\frac{1}{\kappa}\partial_t\right)\theta_c(n,t)=-\frac{1}{\lambda}\sum_{i=1}^{k}w_i\cos\alpha_n a_i\left[H(t-t_{\mathrm{is}})-H(t-t_{\mathrm{ie}})\right] \tag{7}$$

The same described problem could be defined in another way. Instead of surface heat sources, boundary conditions can be written in the form:

$$\lambda\left.\frac{\partial\theta}{\partial z}\right|_{z=0(h)}=-q_i(t),\ i=1,...,k$$

where $q_i(t)$ is the corresponding heat conduction vector component in direction of the z-axis. The differential eq. (2) can be solved using the Fourier transformation, but no heat sources are introduced in equation. Since in this paper a dynamic problem is considered, it is necessary to apply the Laplace transformation solve eq. (7). Laplace transformation:

$$\theta^*(p)=\int_0^\infty\theta(t)\mathrm{e}^{-pt}\mathrm{d}t \tag{8}$$

If the initial condition:

$$\left.\theta\right|_{t=0}=0 \tag{9}$$

the final form of the transformed function $\theta^*_c(n,p)$ is

$$\theta_c^*(n,p)=\frac{\kappa\sum_{i=1}^{k} w_i\cos\alpha_n a_i\left(\mathrm{e}^{-t_{\mathrm{is}}p}-\mathrm{e}^{-t_{\mathrm{ie}}p}\right)}{\lambda(\kappa\alpha_n^2+p)p} \tag{10}$$

In order to obtain an equation that describes the dependence of temperature θ on co-ordinate z and time t, it is necessary to apply the inverse transformations. By applying the inverse transformations, a solution for the temperature field is obtained in the form:

$$\theta(z,t)=\frac{\kappa}{\lambda}\sum_{i=1}^{k} w_i\left[(t-t_{\mathrm{is}})H(t-t_{\mathrm{is}})-(t-t_{\mathrm{ie}})H(t-t_{\mathrm{ie}})\right]+$$
$$+\frac{2}{\lambda h}\sum_{n=1}^{\infty}\sum_{i=1}^{k} w_i\frac{\cos\alpha_n a_i}{\alpha_n^2}\left[\left(1-\mathrm{e}^{-\kappa\alpha_n^2(t-t_{\mathrm{is}})}\right)H(t-t_{\mathrm{is}})-\left(1-\mathrm{e}^{-\kappa\alpha_n^2(t-t_{ie})}\right)H(t-t_{\mathrm{ie}})\right]\cos\alpha_n z \tag{11}$$

Numerical examples

A 100 mm thick steel plate is heated at the upper parallel plane by a 50 kW/m^2 power source. After 500 seconds, the desired maximum temperature change of θ = 100 K is reached and the heat source stops working. If the plate is thermally insulated, the thermal load is evenly distributed over the entire thickness, so that after about 300 seconds (800 seconds since the heating starts) all points have the same temperature of around $\theta = T - T_0 = 68$ K. Material characteristics used in the calculation are characteristic that are commonly used for calculations that involve carbon steel, and are shown in tab. 1.

Table 1. Material characteristics

Material	Elasticity modulus, E [GPa]	Poisson's coefficient, ν	Thermal conductivity, λ [Wm^{-1}K^{-1}]	Specific heat, C [Jkg^{-1}K^{-1}]	Material density, ρ [kgm^{-3}]	Coefficient of thermal expansion, α [K^{-1}]
Carbon steel	210	0.3	50.2	470	7800	1.2 10-5

In fig. 2 the temperatures of the plate layers with co-ordinates z = 0 mm, 25 mm, 50 mm, 75 mm, and 100 mm is shown. It can be seen from the diagram that during this kind of heating, the temperature change across the plate thickness is non-linear (the distance between the lines shown on the diagram is not constant). After the heat source stops working, that is, when a stationary state is established, all points have the same temperature.

Another numerical example is considered as follows. The source with a strength of 50 kW/m^2 is applied to the upper parallel plane and the heat is removed by a sink with a strength

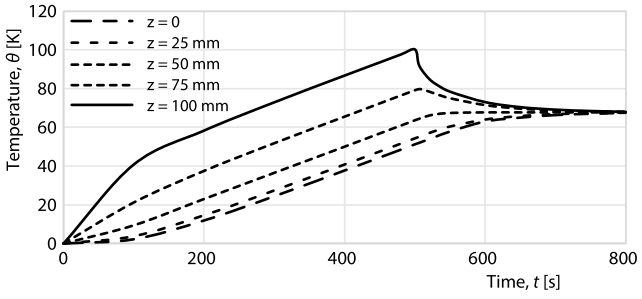

Figure 2. One heat source at the upper parallel plane that works for 500 seconds

of –5 kW/m^2 at the lower side. The corresponding diagram is shown in fig. 3. This diagram represents temperature changes over time for the same values of the z co-ordinate as in the previous numerical example (z = 0 mm, 25 mm, 50 mm, 75 mm, and 100 mm). Analytically obtained layer temperatures are lower than in the previous case, as expected. It can be seen that the temperature change across the plate thickness is non-linear, again.

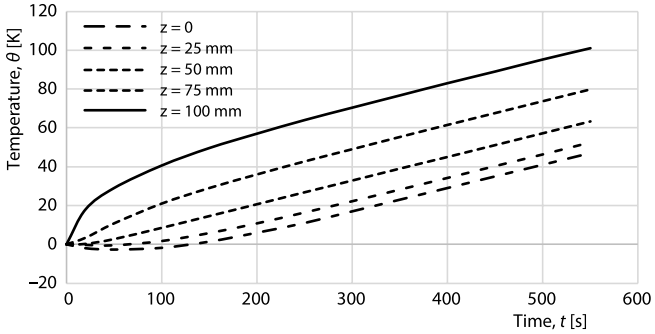

Figure 3. Tho heat sources, one at the upper and the other at the lower parallel plane (w_1 = 50 kW/m^2, w_2 = –5 kWm^{-2}) that work for 550 seconds

In fig. 4 distribution of temperature across the plate thickness after 150 seconds, 300 seconds, and 500 seconds since the beginning of the heat sources (sinks) working is shown. It can be seen from the diagram that temperature distribution across the plate thickness, in this period of time, is non-linear.

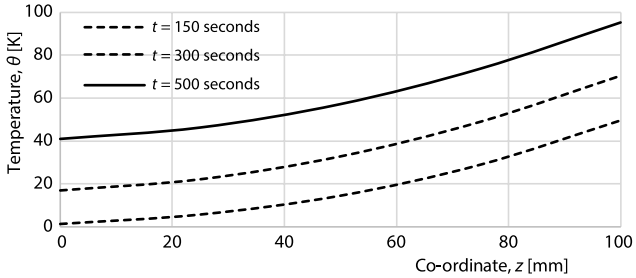

Figure 4. Temperature distribution across the plate thickness during three periods of time – after 150 seconds, 300 seconds, and 500 seconds since the beginning)

In order to achieve a stationary state with a non-linear temperature distribution across the plate thickness, after 550 seconds from the start of heating, the heat source of 50 kW/m^2 stopped working and is replaced by the new source, the third one in eq. (11), of 5 kW/m^2. The new source is installed in order to supply the same amount of heat at the upper side of the plate, and remove the same amount of heat at plates lower side. In fig. 5 the temperature distribution in the newly achieved stationary state is shown. It can be seen that the temperature distribution is still strongly non-linear.

In order to formulate the laws describing this type of plate structures thermal loading, another numerical example are formulated and tested. Four heat sources were installed: the first two with the power of +25 kW/m^2 heat the upper and lower parallel plane for the first 300 seconds, and after that a power source of 5 kW/m^2 acts on the upper plane, and –5 kW/m^2 acts on the lower plane. In fig. 6 distribution of temperature across the plate thickness

(h = 100 mm) is shown, as a function of time. While heating the plate in this way, the temperature field is symmetrical (so, the lines are the same for z = 0 mm, z = 100 mm, z = 25 mm, and z = 75 mm), and also the temperature distribution is non-linear and approximately corresponds to a square parabola line, fig. 7(a).

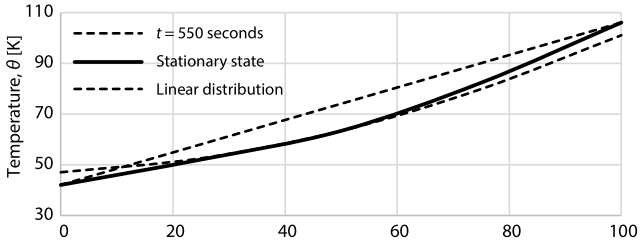

Figure 5. Non-linear temperature distribution in stationary state

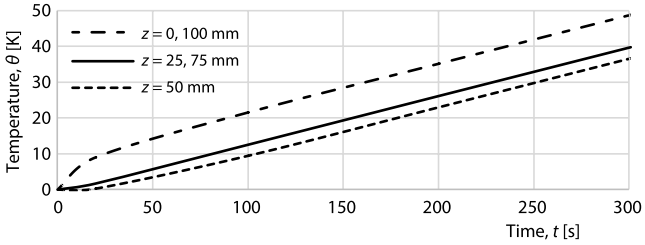

Figure 6. Plate layer temperature while heating (w_1 = 25 kW/m², w_2 = 25 kW/m²)

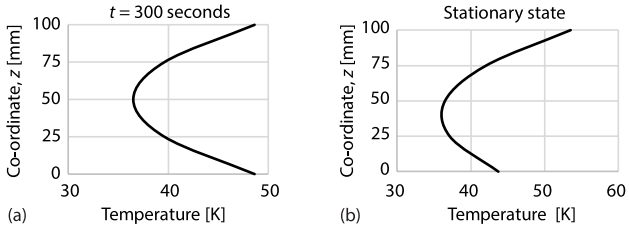

Figure 7. Temperature distribution: (a) after 300 seconds and (b) when stationary state is established

In fig. 7(a) the temperature distribution across the thickness at the end of the heating period is shown. After establishing the stationary state, the temperature distribution shown in fig. 7(b) is obtained. The distribution is not symmetrical and approximately corresponds to a second-degree polynomial.

The diagrams in figs. 3 and 6 show that the lines representing time-temperature dependence in different layers are almost parallel, which means that during heating a constant temperature difference is established between the layers of the plate parallel to (x, y) planes. Hence, conclusions can be made that it is possible to formulate dependence laws. On the basis of these laws the temperature distribution in the plate could be quickly determined at any moment without solving differential equations.

Therefore, it is logical to first examine the influence of only one (1 kW/m²) heat source placed on the upper side of the plate ($z = h$), as follows.

In fig. 8 the change of temperature as a function of time for two plates (plate thickness 50 mm and plate thickness 100 mm) is presented. The lines in the diagram correspond to layers $z = 0$, $z = h/2$, and $z = h$. From this diagram, it can be clearly seen that after some time a linear temperature change is established in the middle plane (layer $z = h/2$), and that the temperature difference between the layers is constant (the lines corresponding to one plate layers are parallel).

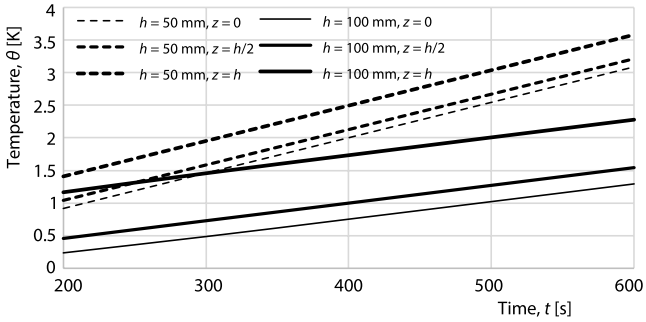

Figure 8. Heating the plate layers; plate thickness 50 mm and plate thickness 100 mm

In fig. 9 middle planes temperature, T_m, change for several plates of different thickness is shown. Temperature change is shown as a function of time. For steel plate elements of relatively small thickness, it can be considered that the change in temperature from the beginning of heating is linear, while with an increase in thickness, linearization is established after a certain relatively short period of time.

For aluminum plates, which have a higher coefficient of thermal conductivity, λ, time for which a linear change is achieved is even shorter. For non-metallic materials with a smaller coefficient λ, that time is slightly longer. For each of these almost straight lines shown in the diagram in fig. 9, the corresponding direction coefficient, K, can be determined. Coefficient K depends only on the plate thickness, h. Since at the beginning of heating, especially for thicker plates, the change is not entirely linear, the direction coefficients were determined after 100 seconds from the start of heating and are shown on diagram in fig. 10. Curve illustrated in fig. 10 is in a hyperbolyc shape type. Since, for small plate thicknesses, funcion has high values alongside with high slope of the curve, part of the curve is illustreted in fig. 10. If the thickness of the plate is expressed in [cm], the direction coefficient, K, can be approximated:

$$K = (27.1/h) \cdot 10^{-3}\ [\mathrm{Ks}^{-1}]$$

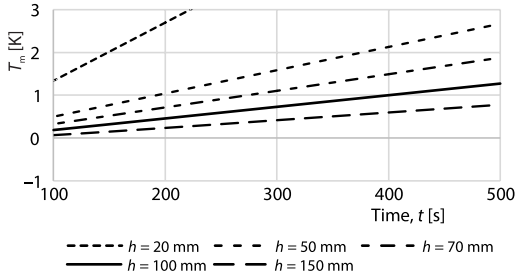

Figure 9. Middle plane temperature, T_m

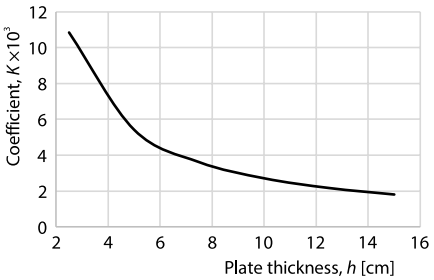

Figure 10. Coefficient K

Since it was already shown that the temperature differences between the layers are constant, it was chosen to determine temperature differences for a moment of 300 seconds. Figure 11 shows: the temperature of the middle plane, T_m, for $t = 300$ seconds; the temperature difference of the upper plate plane and the middle plane $T_u - T_m$, as well as the temperature difference of the middle plane and the lower plane of the plate $T_m - T_d$.

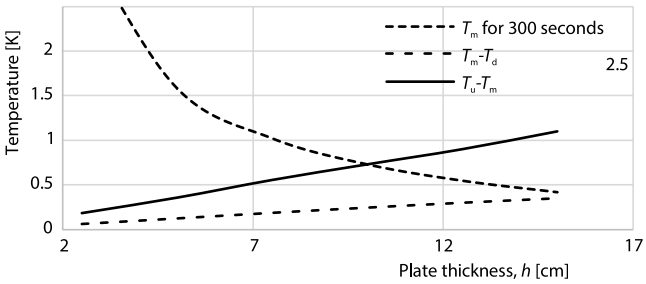

Figure 11. Temperature difference $T_u - T_m$ and $T_m - T_d$ as a function of thickness h

Based on the diagram from figs. 10 and 11, the temperature of the observed element in three characteristic points can be determined. Due to the initial non-linearity, it is suggested that the temperature of the middle plane, T_m, be calculated as $T_m = T_{m300} + K \times (t - 300 \text{ second})$, and only $T_m = K \times t$ can be used for plates up to 100 mm thick. The temperature of the upper plane T_u is calculated as $T_u = T_m + (T_u - T_m)$, and the lower $T_d = T_m - (T_m - T_d)$. If several heat sources (sinks) act on the observed plate element, the characteristic temperatures are obtained by the superposition principle, taking into account the action place of the source and its sign (plus or minus). The practical application of the obtained relations are presented in section *Determining the behavior of thermally loaded structures using FEM*.

The temperatures on the upper and lower parallel plane of the plate are constant

This kind of problem is most often encountered in technical practice, and therefore, it is necessary to first consider it analytically. It starts from the differential eq. (2), to which, in accordance with the given boundary conditions on the upper and lower planes of the plate $\theta(z = h) = \theta_1$, $\theta(z = 0) = \theta_2$, a sinusoidal finite Fourier transformation is applied:

$$\theta_s(n) = \int_0^h \theta(z) \sin \alpha_n z \mathrm{d}z, \ \alpha_n = \frac{n\pi}{h} \tag{12}$$

After applying this transformation, eq. (2) has the form:

$$\alpha_n \left[(-1)^{n+1} \theta_1 + \theta_2 \right] - \alpha_n^2 \theta_s(n,t) - \frac{1}{\kappa} \partial_t \theta_s(n,t) = 0 \tag{13}$$

By applying the Laplace transformation defined by eq. (8), an equation of the transformed function is obtained:

$$\theta_s^*(n,p) = \frac{\kappa \alpha_n \left[(-1)^{n+1} \theta_1 + \theta_2 \right]}{(\kappa \alpha_n^2 + p)p} \tag{14}$$

The solution of a given problem in the form of an infinite series has the form:

$$\theta(z,t)=\frac{2}{h}\sum_{n=1}^{\infty}\frac{(-1)^{n+1}\theta_1+\theta_2}{\alpha_n}\left(1-\mathrm{e}^{-\kappa\alpha_n^2 t}\right)H(t)\sin\alpha_n z,\ 0<z<h,\quad \theta\big|_{z=0}=\theta_2,\ \theta\big|_{z=h}=\theta_1 \tag{15}$$

Numerical example

In fig. 12 the temperature change in the layers of a 100 mm thick plate, with a distance of 25 mm, is shown. For the selected boundary conditions, that the temperature difference between the upper and lower planes of the steel plate is 100 K, it can be seen that the stationary state is established after 250 seconds and that the temperature field along the thickness of the plate has a linear distribution.

In fig. 13 the distribution of temperature across the plate thickness during the establishment of the stationary state is shown. It can be clearly seen that the distribution is already almost linear after 200 seconds. The previous analysis shows that in the majority of thermally loaded machine and other constructions consisting of plate elements, a stationary temperature field is established very quickly, so that the mid-plane temperature and the linear temperature gradient can be obtained from the boundary conditions.

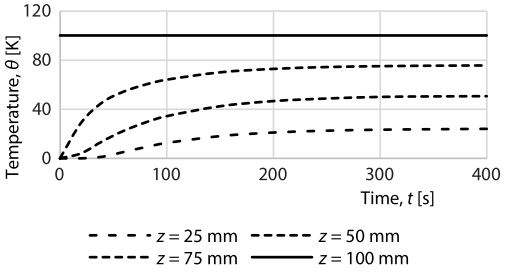

Figure 12. Plate layer temperature as a function of time

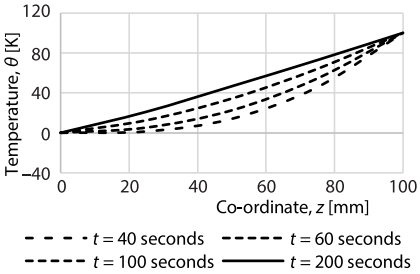

Figure 13. Temperature distribution across the plate thickness t = 40 s, 60 s, 100 s, and 200 s

Determining the behavior of thermally loaded structures using FEM

In order to determine the behavior of geometrically more complex structures that can be represented with finite elements of a thin plate, 2-D finite elements are used. For 2-D finite elements, in addition the membrane equivalent temperature, T_s, a thermal gradient perpendicular to the middle plane, T_g, should be also assigned, software package KOMIPS [23]. The reliability of this finite element is shown in the paper [14]. The co-ordinate system is attached to the middle plane of the plate, and for easier presentation of the equations, the axes are marked according to the tensor notation (x_1, x_2, x_3). Temperature field $\theta(x_1, x_2, x_3, t)$ with non-linear distribution can be described using three values τ_0, τ_1, and τ_2:

$$\theta(x_1,x_2,x_3,t)=\tau_0(x_1,x_2,t)+x_3\tau_1(x_1,x_2,t)+x_3^2\tau_2(x_1,x_2,t) \tag{16}$$

Considering (16), if the eq. (1) is multiplied with $x_3^k (k = 0, 1, 2)$ and an integration the plate thickness is done, three PDE describing the temperature field in a plate could be obtained. Detail explanation of derivation and application of those equations is shown in [24, 25]. For thermal load discussed in section *Surface heat source (sinks) are placef the upper and lower parallel side of the plate*, temperature is:

$$\theta(x_3,t)=\tau_0(t)+x_3\tau_1(t)+x_3^2\tau_2(t)$$

and those equations have the simplified form:

$$-\frac{1}{\kappa}\frac{\partial}{\partial t}\left(\tau_0+\frac{h^2}{12}\tau_2\right)+\frac{1}{h}\left[\frac{\partial\theta}{\partial x_3}\right]_{-\frac{h}{2}}^{h/2}=-\frac{W_0}{h\lambda},\ \left(-\frac{12}{h^2}-\frac{1}{\kappa}\frac{\partial}{\partial t}\right)\tau_1+\frac{12}{h^3}\left[x_3\frac{\partial\theta}{\partial x_3}\right]_{-h/2}^{h/2}=-\frac{12W_1}{h^3\lambda}$$
$$-\frac{1}{\kappa}\frac{\partial}{\partial t}\left(\tau_0+\frac{3h^2}{20}\tau_2\right)-4\tau_2+\frac{12}{h^3}\left[x_3^2\frac{\partial\theta}{\partial x_3}\right]_{-h/2}^{h/2}=-\frac{12W_2}{h^3\lambda},\ W_k=\int_{-h/2}^{h/2}w(x_3,t)x_3^k\,\mathrm{d}x_3 \tag{17}$$

For plate elements thermally loaded in the manner shown in section *Surface heat source (sinks) are placef the upper and lower parallel side of the plate*, it is not necessary to solve these differential equations, but the diagrams shown in figs. 10 and 11 can be used. In order to take into account the part of the thermal load to which the last term in relation (16) corresponds, the linearization:

$$T_s=\tau_0(t)+\frac{1}{h}\int_{-h/2}^{h/2}x_3^2\tau_2(t)\ x_3=\tau_0(t)+\frac{h^2}{12}\tau_2(t),\quad T_g=\tau_1(t) \tag{18}$$

If the temperatures of the three layers, namely T_m, T_u and T_d, are known, then:

$$\tau_0=T_\mathrm{m},\quad \tau_1=\frac{T_\mathrm{u}-T_\mathrm{d}}{h},\quad \tau_2=\frac{2}{h^2}\left(T_\mathrm{u}+T_\mathrm{d}-2T_\mathrm{m}\right)$$

The values entered into numerical (FEM) calculations are:

$$T_s=\frac{4T_\mathrm{m}+T_\mathrm{u}+T_\mathrm{d}}{6},\quad T_\mathrm{g}=\frac{T_\mathrm{u}-T_\mathrm{d}}{h} \tag{19}$$

As an illustration, the strain and stress field is determined for a supported and clamped plate (dimensions 1 m × 1.5 m × 100 mm) that is thermally loaded in the ways shown in section *Surface heat source (sinks) are placef the upper and lower parallel side of the plate*.

Example 1: Three heat sources w_1 = 50 kW/m^2 (550s), w_2 = –5 kW/m^2, w_3 = 5 kW/m^2.

The temperature distribution shown in fig. 4, which corresponds to a time period of 300 seconds from the beginning of the thermal load, can be obtained just by applying the diagram shown in fig. 11. From the diagram, the temperatures for the heat source of unit power are determined, namely: the temperature of the middle plane of 0.73 K, the temperature of the upper plane 0.73 + 0.73 = 1.46 K and the lower plane 0.73 – 0.25 = 0.48 K. When a power source of 50 kWm^2 is applied on the upper plane and –5 kW/m^2 on the lower plane, then:

$$T_\mathrm{m}=0.73\times50-0.73\times5=3\ 2.85\ \mathrm{K}$$
$$T_\mathrm{u}=1.46\times50-0.48\times5=70.6\ \mathrm{K}$$
$$T_\mathrm{d}=0.48\times50-1.46\times5=16.7\ \mathrm{K}$$

Values for numerical (FEM) calculation are: T_s = 36.45 K and T_g = 5.39 K/cm.

In order to obtain the temperature values at the end of the heating of 550 seconds to the previously determined value for t = 300 seconds, additional K × (550 – 300) × (50 – 5) = 26.73 K should be added. At the end of the heating, the temperatures are: T_m = 59.58 K, and T_u = 97.33 K, T_d = 43.43 K which corresponds with the diagram shown in fig. 4, obtained by solving the differential eq. (2). The parameters for the finite element calculation are: T_s = 63.18 K and T_g = 5.39 K/cm.

In fig. 14 the deformation and distribution of equivalent stresses for a plate supported in all three directions after heating for 300 seconds are shown. For the clamped plate after 550 seconds, the following stress values are obtained: if both parameters T_s i T_g are included,

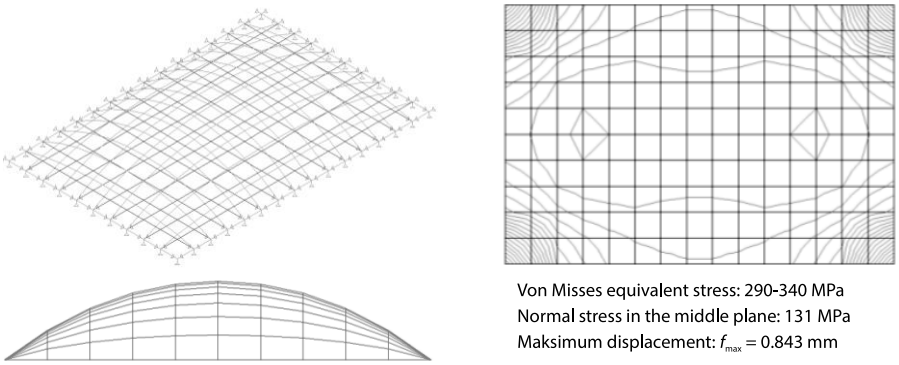

Figure 14. Deformation and stresses of the supported plate t = 300 seconds

the equivalent stress σ_{eq} is 325 MPa, the percentage of membrane stress is 70.1%, and bending stress is 29.2%; when only T_s is included σ_{eq} = 227 MPa (membrane stress), when only T_g σ_{eq}= 97 MPa (bending stress).

Example 2: Four heat sources $w_1 = w_2$ = 25 kW/m^2 (300 seconds), w_3 = 5 kW/m^2, w_4 = –5 kW/m^2.

Based on the diagram shown in fig. 11, after 300 seconds, the temperature characteristic of the three layers is T_m = 0.73 × 25 + 0.73 × 25 = 36.5 K, and $T_u = T_d$ = 1.46 × 25 + 0.48 × 25 = 48.5 K, which matches the diagram shown in fig. 9(a). The parameters for the finite element calculation are T_s = 40.5 K and T_g = 0 K/cm, hence there is no plate bending.

In order to obtain the temperature distribution in the stationary state, these values are taken as initial and the influence of two sources of ±5 kW/m^2 is added. For the sake of simplicity, the diagram from fig. 11 is used again and the temperatures of the layers at the moment of 600 seconds from the start of heating (300 seconds from the introduction of new heat sources) are determined. The temperatures of the layers are T_m = 36.5 + 0.73 × 5 – 0.73 × 5 =36.5 K, T_u = 48.5 + 1.46 × 5 – 0.48 × 5 = 53.4 K, and T_d = 48.5 + 0.48 × 5 – 1.46 × 5 = 43.6 K. It is clear that this corresponds to the distribution shown in fig. 9(b). The parameters for the finite element calculation are: T_s = 40.5K i T_g = 0.98 K/cm.

For a freely supported plane due to stress concentration at the corners equivalent stress is σ_{eq}= 29 – 43 MPa. For a plate with supports in all three directions deflection is f_{max} = 0.153 mm, normal stresses in the middle plane are 146 MPa, σ_{eq} = 175 MPa, membrane stresses have the share of 82.56%, and bending stresses of 17.44%. The clamped plate has stress of σ_{eq}=163 MPa.

Conclusion

In this paper plate elements thermally insulated along the sides and loaded with heat sources (sinks) with limited action on the frontal sides are analyzed. The problem is first mathematically defined using the appropriate differential equation, and then solved in a closed analytical form using the technique of integral transformations (Fourier and Laplace). By considering the obtained solutions, it can be concluded that the heat load set in this way for metal plate elements very quickly gives a linear dependence of the temperature of the middle plane as a function of time, and that the temperature differences between the layers are almost constant. Based on those conclusions, two diagrams corresponding to heat source of unit intensity were

formed, on the basis of which, without solving differential equations, the temperature of the three basic layers can be easily determined at any time of heating or cooling of the observed element. Diagrams are shown for steel plate, and can be formed in the same way for any other material. The non-linear temperature distribution is adapted to the calculation using the FEM, where for more complicated geometry, 2-D finite elements can be used instead of 3-D elements. Hence, numerical calculations are simplified by this method.

Acknowledgment

This work was supported by the Ministry of Science, Technological Development and Innovation, Republic of Serbia (Project No. 451-03-65/2024-03/200105 from 5 February 2024).

Nomenclature

$H(t)$ – Heaviside function
h – plate thickness, [m]
K – temperature direction coefficient, [Ks^{-1}]
p – Laplace parameter
T – temperature, [°C or K]
T_g – temperature gradient, [Km^{-1}]
T_s – equivalent temperature of the membrane
t – time, [second]
∂t – time derivative
w_i – power of surface sources (sinks), [Wm^{-2}]

Greek symbols

δ – Dirac function
θ – temperature field (change in temperature comparing to its natural state), [°C or K]
κ – coefficient of thermal intensity, [m^2s^{-1}]
λ – thermal conductivity, [$Wm^{-1}K^{-1}$]
σ – stress, [Pa]

Subscripts

d – down
eq – equivalent
m – middle
u – upper

References

[1] Seddiq, M., Maerefat, M., Analytical Solution for Heat Transfer Problem in A Cross-Flow Plate Heat Exchanger, *International Journal of Heat and Mass Transfer*, *163* (2020), 120410
[2] Gaćeša, B., *et al*., Influence of furnace tube shape on thermal strain of fire-tube boilers, *Thermal Science*, *18* (2014), Suppl. 1, pp. S39-S47
[3] Rajić, M., *et al*., Construction Optimization of Hot Water Fire-Tube Boiler Using Thermomechanical Finite Element Analysis, *Thermal Science*, *22* (2018), Suppl. 5, pp. S1511-S1523
[4] Lindgren, L.-E., *et al*., Modelling of Thermal Stresses in Low Alloy Steels, *Journal of Thermal Stresses 42* (2019), 3, pp. 1-9
[5] Hemanth, J., Yogesh, K. B., Finite Element Analysis (FEA) and Thermal Gradient of a Solid Rectangular Fin with Embossing's for Aerospace Applications, *Advances in Aerospace Science and Technology*, *3* (2018), 3, pp. 49-60
[6] Shi, Y., *et al*., Temperature Gradient Mechanism in Laser Forming of Thin Plates, *Optics and Laser Technology*, *39* (2007), 4, pp. 858-863
[7] Murphy, K., Ferreira, D., Thermal Buckling of Rectangular Plates, *International Journal of Solids and Structures*, *38* (2001), 22-23, pp. 3979-3994
[8] Dhakate., T, *et al*., Analysis of Thermal-Bending Stresses in Simply Supported Annular Sector Plate, *Journal of Solid Mechanics*, *11* (2019), 4, pp. 724-735
[9] Khazaeinejad, P., *et al*., Temperature-Dependent Non-Linear Behaviour of Thin Rectangular Plates Exposed to through-Depth Thermal Gradients, Composite Structures, *132* (2015), Nov., pp. 652-664
[10] Perkowski, S., *et al*., Axisymmetric Stationary Heat Conduction Problem For Half-Space With Temperature-Dependent Properties, *Thermal Science*, *24* (2020), 3B, pp. 2137-2150
[11] Vaghefi, R., The 3-D Temperature Dependent Thermo-Elastoplastic Bending Analysis of Functionally Graded Skew Plates Using a Novel Meshless Approach, *Aerospace Science and Technology, 104* (2020), 105916
[12] Sator, L., *et al*., Bending of FGM Plates under Thermal Load: Classical Thermoelasticity Analysis by a Meshless Method, *Composites Part B*, *146* (2018), Aug., pp. 176-188

[13] Allam, M., Tayel, I., Thermal Effects on Transverse Vibrations of Non-Homogeneous Rectangular Thin Plate Subjected to A Known Temperature Distribution, *Transactions of Canadian Society for Mechanical Engineerin*g, *44* (2020), 3
[14] Milošević-Mitić, V., *et al*., The Influence of Temperature Gradient on the Thin Plates Bending, *FME Transactions*, *52* (2024), 1, pp. 128-135
[15] Shen, H., *et al*., Study on Temperature Field Induced in High Frequency Induction Heating, *Acta Metallurgica Sinca*, *19* (2006), 3, pp. 190-196
[16] Milošević-Mitić V., *et al.*, Dynamic Temperature Field in the Ferromagnetic Plate Induced by Moving High Frequency Inductor, *Thermal Science*, *18* (2014), Suppl. 1, pp. S49-58
[17] Musii, R., *et al*., Analysis of Varying Temperature Regimed in a Conductive Strip during Induction Heating under a Quasi-Steady Electromagnetic field, *Energies*, *17* (2024), 366
[18] Musii, R., *et al.*, Modelling of the Temperature Regimes in a Layered Bimetallic Plate under Short – Term Induction Heating, *Energies*, *16* (2023), 4980
[19] Milošević-Mitić V., *et al.*, Influence of Specific Electrical Resistance on the Heating of Metal Plates Exposed to High-Frequency Electromagnetic Waves, *Thermal Science*, *27* (2023), 5, pp. 3649-3658
[20] He, J.-H., *et al*., Beyond Laplace and Fourier Transforms-Challenges and Future Prospects, *Thermal Science*, *27* (2023), 6B, pp. 5075-5089
[21] Abouelregal, A. E., *et al*., Temperature-Dependent Physical Characteristics of the Rotating Non-Local Nanobeams Subjected to a Varying Heat Source and A Dynamic Load, Facta Universitatis: *Series Mechanical Engineering*, *19* (2021), 4, pp. 633-656
[22] Thakur, P., Steady Thermal Stress and Strain Rates in a Circular Cylinder With Non-Homogeneous Compressibility Subjected to Thermal Load, *Thermal Science*, *18* (2014) Suppl. 1, pp. S81-S92
[23] Maneski, T., *Computer Modelling and Structure Analysis*, Faculty of Mechanical Engineering, University of Belgrade, Belgrade, Serbia, 2000
[24] Milošević-Mitić V., Maneski T., The influence of the Non-Linear Temperature Field on the Behavior of the Metallic Plate Induced by Two Electromagnetic Waves Obtained by GSP, Facta Universitatis: Series Mechanics, A*utomatic Control and Robotics*, *3* (2003), 15, pp. 1113-1120
[25] Milošević-Mitić V., *et al.*, Dynamic Non-Linear Temperature Field in a Ferromagnetic Plate Induced by High Frequency Electromagnetic Waves, *Strojarstvo*, *52* (2010), 2, pp. 115-124

Paper submitted: July 5, 2024
Paper revised: November 6, 2024
Paper accepted: November 12, 2024